Separation Science and Technology
Publication details, including instructions for authors and subscription information:
http://www.informaworld.com/smpp/title~content=t713708471

A Stefan-Maxwell Analysis of Protein Transport in Porous Membranes

Bruce C. Robertson[a]; Andrew L. Zydney[a]
[a] Department of Chemical Engineering, University of Delaware, Newark, DE

To cite this Article Robertson, Bruce C. and Zydney, Andrew L.(1988) 'A Stefan-Maxwell Analysis of Protein Transport in Porous Membranes', Separation Science and Technology, 23: 12, 1799 — 1811
To link to this Article: DOI: 10.1080/01496398808075664
URL: http://dx.doi.org/10.1080/01496398808075664

SEPARATION SCIENCE AND TECHNOLOGY, 23(12&13), pp. 1799-1811, 1988

A Stefan-Maxwell Analysis of Protein Transport in Porous Membranes

Bruce C. Robertson
Andrew L. Zydney
Department of Chemical Engineering
University of Delaware
Newark, DE 19716

ABSTRACT

The Stefan-Maxwell multicomponent diffusion equations were used to characterize albumin transport in ultrafiltration membranes in both an unstirred batch filtration device and a well-stirred diffusion cell. We developed a theoretical model for ultrafiltrate flux and concentration in the filtration device that explicitly incorporates the effects of protein polarization, protein osmotic pressure, and a flux-dependent sieving coefficient. Experimental data were in good agreement with model predictions, providing quantitative evidence for the predicted dependence of the apparent sieving coefficient on flux. Experimental data in the diffusion cell indicate that the effective albumin diffusivity in the 50,000 molecular weight cut-off membranes was four orders of magnitude less than the Brownian motion value. The Stefan-Maxwell diffusivities evaluated independently in the two experimental systems were in excellent agreement, indicating the general applicability of the Stefan-Maxwell approach to protein transport in ultrafiltration membranes.

INTRODUCTION

Membrane separation processes are becoming increasingly attractive for a variety of industrial, biochemical, and biomedical applications. In general, these processes are governed by both bulk (concentration polarization) and membrane (sieving and diffusion) transport phenomena. The coupling

between the bulk and membrane transport has posed significant problems in (i) evaluating intrinsic membrane properties, and (ii) extrapolating results from one experimental system to another or from laboratory to industrial scale devices. In this study, we investigated the transport of albumin in 50,000 molecular weight cut off membranes using both an unstirred batch filtration cell and a well-stirred diffusion cell. We developed theoretical models for both bulk and membrane transport in these systems and then used these models to evaluate intrinsic membrane transport properties which are shown to be independent of both flow rate and experimental geometry.

MATERIALS AND METHODS

All experiments were performed with bovine serum albumin (Cohn Fraction V, Sigma Chemicals) in 0.15M NaCl. BSA concentrations were measured spectrophotometrically. Flat sheet polyethersulfone NOVA-50 membranes with 50,000 molecular weight cut off, provided by Filtron Corporation (Clinton, MA), were used in both the filtration and diffusion experiments.

Filtration Experiments

Filtration experiments were performed in an unstirred, vacuum-driven, batch cell (Figure 1). Membranes were supported in a 47 mm diameter chamber providing an effective membrane surface area of 13.9 cm^2. Prior to each experiment, the membrane hydraulic permeability was evaluated from saline flux vs. pressure drop measurements. All sieving experiments were carried out with an applied pressure of 200 mm Hg which was maintained to within 3%. Details of the experimental protocol are described elsewhere (1).

Diffusion Experiments

Protein transport was also analyzed using a well-stirred diffusion cell (Figure 2) which was a modification of the apparatus used by Keller et al. (2) and Scattergood and Lightfoot (3). Two identical plexiglas chambers, each with 7.5 cm^3 total volume, were separated by a NOVA-50 membrane with an effective cross-sectional area of 3.14 cm^2. Each chamber was stirred at a constant speed of approximately 100 rpm to eliminate bulk concentration gradients. At the start of a run, the two chambers were filled with protein solution of identical concentrations. A small volume (approximately 100 μL) of ^{125}I labeled bovine serum albumin (New England Nuclear, Boston, MA) was then injected through the syringe port on one side. Protein diffusive flux across the membrane was evaluated by monitoring the activity in both chambers as a function of time, thus enabling us to calculate protein diffusivities in the membrane. Additional details on the experimental apparatus and procedure are discussed in a forthcoming study (4).

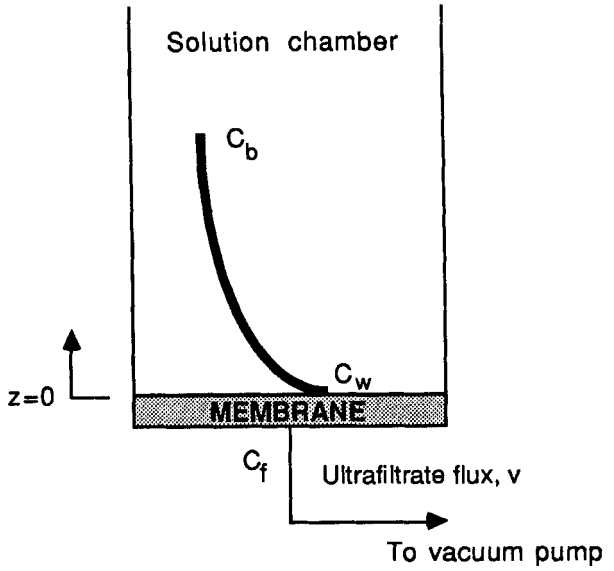

Fig. 1. Schematic diagram of unstirred filtration cell showing polarization

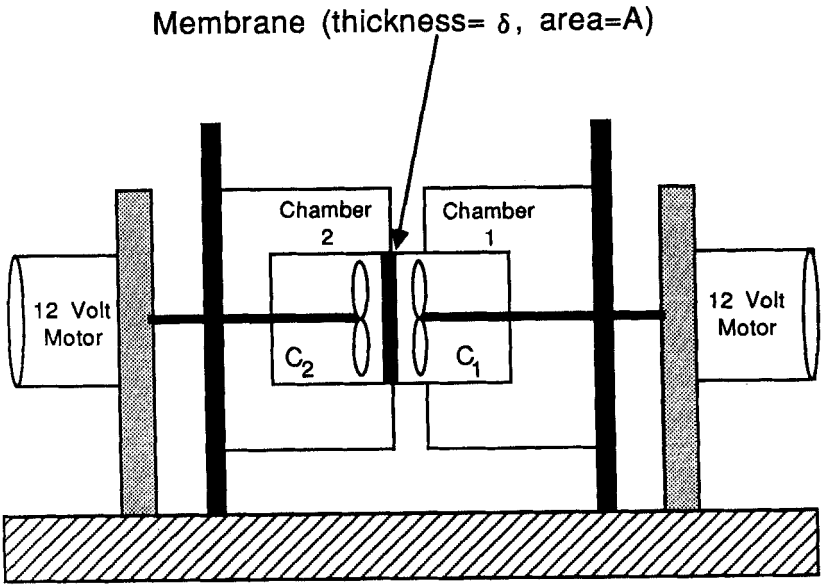

Fig. 2. Schematic diagram of the diffusion cell

THEORY

In general, there are two approaches used to describe solute transport in membranes: the Kedem-Katchalsky analysis (5, 6) and the Stefan-Maxwell multicomponent diffusion analysis (7). The relationship between these approaches has been described by Lightfoot (7) and Lewellen (8). In this study, we have employed the Stefan-Maxwell analysis since it has a more rigorous theoretical basis and the resulting equations can be more easily applied to different geometries and to systems with more than one solute.

Membrane Transport

In the Stefan-Maxwell analysis the membrane is treated as a diffusing species constrained to zero velocity and near-zero concentration gradients (3, 7). The one-dimensional Stefan-Maxwell equations in the membrane (m) for protein (p) and solvent (s) are

$$\frac{\bar{V}_p}{RT}\frac{dP}{dz} + \frac{d}{dz}\ln(x_p\gamma_p) = \frac{1}{C_pD_{ps}}(x_pN_s - x_sN_p) - \frac{1}{C_pD_{pm}}x_mN_p \quad (1)$$

$$\frac{\bar{V}_s}{RT}\frac{dP}{dz} + \frac{d}{dz}\ln(x_s\gamma_s) = \frac{1}{C_sD_{ps}}(x_sN_p - x_pN_s) - \frac{1}{C_sD_{sm}}x_mN_s \quad (2)$$

where γ_i is the activity coefficient for component i. The phenomenological coefficients, D_{ij}, are independent except for the symmetry condition, $D_{ij} = D_{ji}$. For gases at moderate pressures, the D_{ij} are identical to the corresponding binary diffusion coefficients (8, 9, 10). Although, in general, the D_{ij} are functions of local pressure, temperature, and composition, the set of parameters D_{ps}, x_m/D_{pm}, and x_m/D_{sm} is relatively insensitive to variations in pressure and composition (7). These three parameters thus provide a convenient description of the transport properties of the protein/membrane system independent of flow rate and experimental configuration.

For our subsequent analysis, it is convenient to rewrite the flux equations in terms of the ultrafiltrate velocity, v,

$$v = \bar{V}_sN_s + \bar{V}_pN_p \quad (3)$$

In the dilute solution limit the flux equations become (7, 8, 11)

$$v = -\frac{1}{C}\frac{D_{sm}}{RT}\frac{1}{x_m}\left[\frac{dP}{dz} - CRT\left(1 - \frac{D_2}{D_1}\right)\frac{d}{dz}\ln(x_s\gamma_s)\right] \quad (4)$$

$$N_p = \frac{D_2}{D_1}x_pCv - D_2Cx_p\frac{d}{dz}\ln(x_p\gamma_p) \quad (5)$$

where

$$\frac{1}{D_1} = \frac{1}{D_{ps}} + C\bar{V}_p\frac{x_m}{D_{sm}} \quad (6)$$

and

$$\frac{1}{D_2} = \frac{x_s}{D_{ps}} + \frac{x_m}{D_{pm}} \tag{7}$$

In the development leading to Eqs. (4) and (5) we have made use of the Gibbs-Duhem relation

$$x_p \frac{d}{dz} \ln(x_p \gamma_p) + x_s \frac{d}{dz} \ln(x_s \gamma_s) = 0 \tag{8}$$

where the membrane phase is treated as being thermodynamically binary since its equilibrium state is fixed by that of the binary external phase (7). Eqs. (4) and (5) are analogous to the differential form of the Kedem-Katchalsky equations with σ, the Staverman reflection coefficient, given as

$$\sigma = \left(1 - \frac{D_2}{D_1}\right) \tag{9}$$

Batch Filtration

For the system depicted schematically in Figure 1, the one-dimensional species continuity equation is (assuming a constant protein diffusivity, D)

$$\frac{\partial C}{\partial t} + v \frac{\partial C}{\partial z} = D \frac{\partial^2 C}{\partial z^2} \tag{10}$$

subject to the boundary conditions

$$vC - D \frac{\partial C}{\partial z} = vC_f = N_p(\text{membrane}) \qquad \text{at} \qquad z = 0 \tag{11}$$

$$C = C_b \qquad \text{at} \qquad z = \infty \tag{12}$$

and initial condition

$$C = C_b \qquad \text{at} \qquad t = 0 \tag{13}$$

where C_f and C_b are the filtrate and bulk protein concentrations, respectively. The ultrafiltrate velocity is evaluated by integrating Eq. (4) across the membrane of thickness δ to give

$$v = -\frac{D_{sm}}{x_m} \frac{1}{\delta CRT} [\Delta P - \sigma \Delta \pi] = -L_p [\Delta P - \sigma \Delta \pi] \tag{14}$$

where L_p is the hydraulic permeability and

$$\Delta \pi = \pi|_{C_w} - \pi|_{C_f} = CRT[\ln(x_w \gamma_w) - \ln(x_f \gamma_f)] \tag{15}$$

As we will show the protein flux in the membrane, N_p, can be expressed in terms of the protein concentration at the membrane surface, $C_w(t)$, through the apparent sieving coefficient, S_a

$$N_p(\text{membrane}) = vC_f = vC_wS_a \tag{16}$$

where

$$S_a = \frac{C_f}{C_w} \tag{17}$$

The apparent sieving coefficient is often assumed to depend only on the properties of the membrane and the solute. In reality, S_a is also a function of the convective and diffusive fluxes of solute through the membrane. In what follows, an explicit relationship between C_f and C_w is developed by solving the Stefan-Maxwell equations for the protein concentration profile in the membrane.

Under conditions of dilute solution, Eq. (5) can be written as

$$\frac{dx_p}{dz} = \frac{1}{D_1}x_pv - \frac{1}{CD_2}N_p \tag{18}$$

with D_1 and D_2 given by Eqs. (6) and (7), respectively. Eq. (18) can be integrated across the membrane using the continuity equations for protein and solvent (7)

$$N_p = \text{constant} \tag{19}$$

$$N_s = \text{constant} \tag{20}$$

to give

$$x_f\frac{D_1}{D_2} + \left(Kx_w - \frac{D_1}{D_2}x_f\right)\exp\left(-\frac{\delta}{D_1}v\right) = Kx_f \tag{21}$$

In deriving Eq. (21) we have applied equilibrium conditions at the upper ($z = 0$) and lower ($z = -\delta$) surfaces of the membrane

$$K = \frac{x_p(\text{membrane})}{x_p(\text{solution})} = \frac{\gamma_p(\text{solution})}{\gamma_p(\text{membrane})} \tag{22}$$

where K is the equilibrium partition coefficient. We have also used the relationship between the filtrate concentration and the solute and solvent fluxes (7)

$$x_f = \frac{N_p}{N_p + N_s} \approx \frac{N_p}{N_s} \tag{23}$$

where the final expression is valid for sufficiently dilute solutions. Under these conditions, the ultrafiltrate velocity is given by $v = N_s/C$ and the flux of protein is expressed as

$$N_p = x_fN_s = vC_f \tag{24}$$

as previously stated in Eq. (16).

Eq. (21) can be used to evaluate the apparent sieving coefficient in terms of the Stefan-Maxwell diffusivities and the filtration velocity, v, as

$$S_a = \frac{C_f}{C_w} = \frac{x_f}{x_w} = \frac{K\frac{D_2}{D_1}F}{K\frac{D_2}{D_1} + F - 1} \tag{25}$$

where

$$F = \exp\left(-\frac{\delta}{D_1}v\right) \tag{26}$$

Since the ultrafiltrate flux in our coordinate system is negative, S_a approaches its limiting value

$$S_a = K\frac{D_2}{D_1} \tag{27}$$

at high fluxes (large F) and increases as the flux decreases. The dependence of S_a on v is also discussed by Spiegler and Kedem (6) and Lysaght (12).

Eqs. (10) through (16), with S_a given by Eqs. (25) and (26), completely describe protein and solvent transport in the batch filtration system. We have developed an integral solution to these equations assuming a cubic polynomial in z for the concentration profile (11). The result can be expressed as

$$\frac{dC_w}{dt} = \frac{1}{\alpha}\frac{v}{D}[C_b - S_aC_w] \tag{28}$$

where

$$\alpha = \frac{(C_w - C_b)^2}{C_w^2v^2(1 - S_a)^2}\left[v(1 - S_a) - vC_w\frac{dS_a}{dv}\frac{dv}{dC_w} + C_w(1 - S_a)\frac{dv}{dC_w}\right]$$

$$+\frac{2(C_w - C_b)}{C_wv(1 - S_a)} \tag{29}$$

$C_w(t)$ is evaluated by numerically integrating Eqs. (28) and (29) with the albumin osmotic pressure evaluated from the data of Vilker et al. (13) using a cubic virial expansion in concentration (with virial coefficients $B_2 = 9.22 \times 10^{-3}$ L/g, $B_3 = 3.03 \times 10^{-5}$ L^2/g^2). The term dv/dC_w in Eq. (29) is evaluated analytically using Eqs. (14), (15), and (25) and dS_a/dv is evaluated from Eqs. (25) and (26).

Diffusion Cell

Experimental data in the diffusion cell were analyzed using the procedure outlined by Scattergood and Lightfoot (3) and Keller et al. (2). The flux

of radiolabeled protein (N_{p^*}) can be evaluated using the Stefan-Maxwell analysis

$$\frac{d}{dz}\ln(x_{p^*}\gamma_{p^*}) = \frac{1}{C_{p^*}D_{pp^*}}(x_{p^*}N_p - x_pN_{p^*}) - \frac{1}{C_{p^*}D_{p^*s}}(x_sN_{p^*}) - \frac{1}{C_{p^*}D_{p^*m}}(x_mN_{p^*}) \tag{30}$$

where $N_s = 0$ since x_s is constant throughout the system and $dP/dz = 0$.

The flux of labeled protein (N_{p^*}) is equal, but opposite, to that of the unlabeled protein, $N_{p^*} = -N_p$. Since the labeled and unlabeled protein are essentially indistinguishable in terms of their thermodynamic behavior we can write $\gamma_{p^*} = \gamma_p$. Since the total protein concentration $x_p + x_{p^*}$ is constant throughout the system, the activity coefficient, γ_{p^*} is independent of position and Eq. (30) can be solved for the protein flux to yield

$$N_{p^*} = -CD_{\text{eff}}\frac{dx_{p^*}}{dz} \tag{31}$$

where

$$\frac{1}{D_{\text{eff}}} - \frac{x_s}{D_{ps}} + \frac{x_m}{D_{pm}} + \frac{x_p + x_{p^*}}{D_{pp^*}} = \frac{1}{D_2} + \frac{x_p + x_{p^*}}{D_{pp^*}} \tag{32}$$

In writing Eq. (32), the radiolabeled protein diffusivities, D_{p^*s} and D_{p^*m}, have been replaced by D_{ps} and D_{pm} since the labeled and unlabeled proteins have essentially identical transport properties in the membrane. Since the solvent, membrane, and total protein mole fractions do not vary with time, D_{eff} is a constant for a given experimental run. The protein mass balances in each chamber can be integrated directly, using Eq. (31), assuming quasi-steady operation, to give (3)

$$\ln\left[\frac{(C_1 - C_2)_t}{(C_1 - C_2)_0}\right] = -\frac{KD_{\text{eff}}A}{\delta}\left(\frac{1}{V_1} + \frac{1}{V_2}\right)t \tag{33}$$

where C_1 and C_2 refer to the labeled protein concentration in the two chambers of the diffusion cell and A is the membrane cross-sectional area. In our experiments, the volumes of the two chambers were equal, $V_1 = V_2$. Bulk concentration gradients were shown to be negligible under our experimental conditions (4). The product KD_{eff} can then be evaluated directly from data for C_1 and C_2 as a function of time.

RESULTS AND DISCUSSION

Experimental data for the ultrafiltrate velocity and for the ratio of filtrate to bulk protein concentration are shown as a function of time in the top

and bottom panels of Figure 3, respectively. Results are shown for a bulk albumin concentration of 5.6 g/L and a membrane hydraulic permeability of $L_p = 6 \times 10^{-6}$ cm/sec/mm Hg (determined from saline flux data). The solid and dashed curves represent the model predictions, evaluated by numerically integrating Eqs. (28) and (29). The equilbrium partition coefficient, K, was estimated as approximately 0.1 (11) using the first term the virial expansion for K in concentration (14)

$$K = \frac{V'}{V_{\text{pore}}} \tag{34}$$

where V' is the volume of the pores accessible to the centers of the molecules (assumed spherical) and V_{pore} is the total pore volume. The best-fit values for KD_2/D_1 and δ/D_1 were determined by minimizing the sum of the squared residuals between experimental and predicted values of C_f/C_b and v. This analysis gave the values $KD_2/D_1 = 0.010 \pm 0.001$ and $\delta/D_1 = 1.7 \pm 0.1 \times 10^4$ sec/cm. Attempts to evaluate all three parameters (KD_2/D_1, δ/D_1, and K) from the filtration data led to physically inconsistent results due to the high correlation among these three parameters. The model predictions are in good agreement with the experimental data for C_f/C_b, with a mean square deviation between predicted and experimental values of 8%.

Both the model predictions and experimental data show that C_f/C_b rises very rapidly at short times ($t < 50$ minutes) and then increases more gradually for times greater than 50 minutes. This initial rise is due to bulk concentration polarization effects with the wall concentration rapidly approaching its asymptotic value $C^\dagger$ for which $\Delta P - \sigma\Delta\pi \rightarrow 0$. For these experimental conditions, with the best-fit values for KD_2/D_1 and δ/D_1 (corresponding to $\sigma = 0.9$), the asymptotic concentration is $C^\dagger \approx 200$ g/L. The wall concentration has attained 98% of this value at $t = 50$ minutes while the apparent sieving coefficient is only slightly greater than the high-flux value, $S_a = KD_2/D_1 = 0.010$, at this time. At longer times ($t > 50$ minutes), the ultrafiltrate flux becomes small enough that diffusive transport of albumin through the membrane becomes important. Under these conditions, the apparent sieving coefficient is greater than the high-flux asymptote as diffusion tends to reduce the concentration gradient across the membrane. The gradual increase in C_f/C_b at longer times reflects the rise in S_a associated with this decrease in ultrafiltrate flux. By the end of the experiment ($t = 520$ minutes), S_a is 0.023 according to the model, more than twice the high-flux value. If S_a were assumed to be constant, as is often done in such systems, it becomes impossible to accurately describe the C_f/C_b data in Figure 3.

The solid and dashed curves in Figure 3 represent model predictions evaluated with two different values of the bulk Brownian diffusion coefficient: the literature estimate under our experimental conditions, $D = 6 \times 10^{-7}$ cm^2/sec (2) and $D = 30 \times 10^{-7}$ cm^2/sec as suggested by Vilker et al. (15).

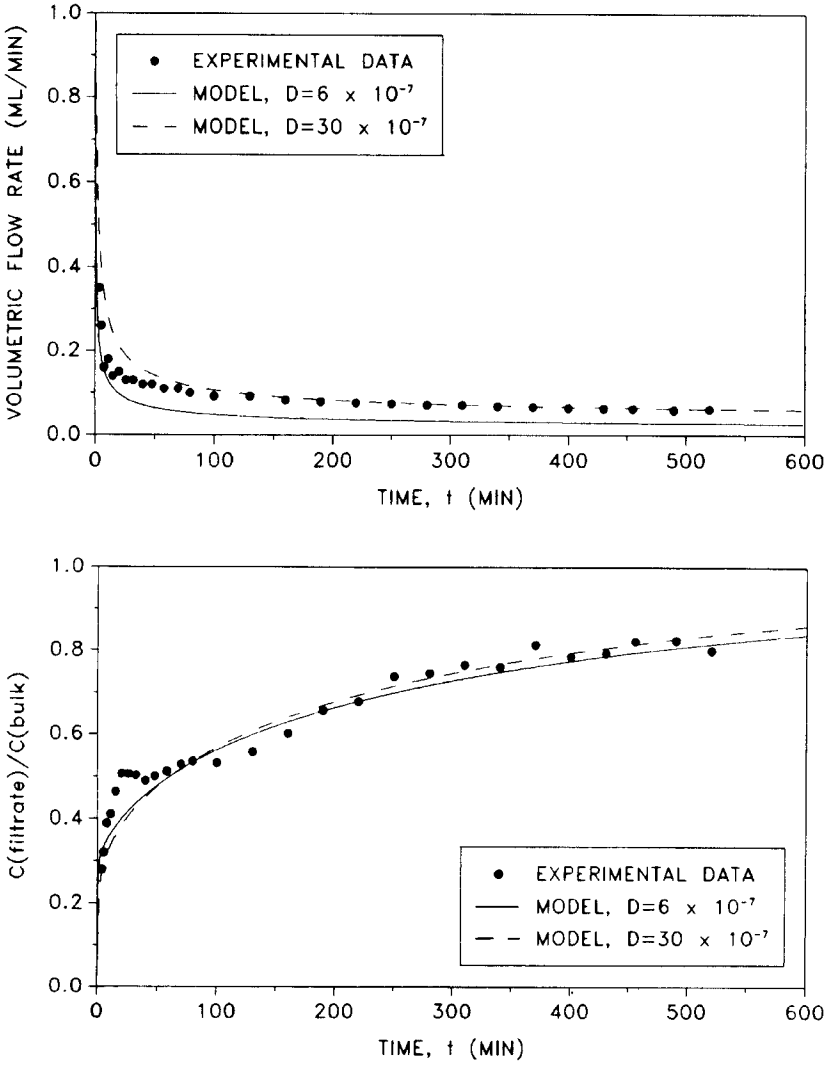

Fig. 3. Data for the ultrafiltrate flux (top) and the ratio of the filtrate to bulk concentrations (bottom) as functions of time. Solid and dashed curves are model predictions from integration of Eq. (28).
Solid curve: ($D = 6 \times 10^{-7}$ cm^2/sec) $\frac{KD_2}{D_1} = 0.010$, $\frac{\delta}{D_1} = 17{,}000$.
Dashed curve: ($D = 30 \times 10^{-7}$ cm^2/sec) $\frac{KD_2}{D_1} = 0.010$, $\frac{\delta}{D_1} = 7000$.

Both curves are in good agreement with the sieving data in the lower panel, but the dashed curve ($D = 30 \times 10^{-7}$ cm^2/sec) is in significantly better agreement with the flux data. This type of discrepancy was also described by Vilker et al. (15) in their analysis of albumin ultrafiltration in an unstirred batch cell and they attributed it to the effect of diffusion potentials. We also explored the effect that varying KD_2/D_1, δ/D_1, and K had on the predicted ultrafiltrate flux, but no combination of these could provide an adequate fit to the flux data. The relative insensitivity of the flux to these parameters is in agreement with the long-time solution for v developed by Vilker et al. (15)

$$v = v_o \left(\frac{D}{t}\right)^{\frac{1}{2}} \tag{35}$$

for a highly-rejecting membrane with constant S_a. Their study showed that v_o is a function only of $C^\dagger$, C_b, and σ, and has only a weak dependence on σ when $C^\dagger/C_b >> 1$ as is the case in our experiments.

The experimental results for KD_2/D_1 and δ/D_1 can be used, in conjunction with the measured hydraulic permeability, to evaluate the three phenomenological coefficients describing membrane transport. Eqs. (6) and (7) give $D_{ps} = 4.0 \times 10^{-9}$ cm^2/sec, $D_{pm}/x_m = 3.2 \times 10^{-10}$ cm^2/sec, and $D_{sm}/x_m = 3.1 \times 10^{-4}$ cm^2/sec. D_{pm} is six orders of magnitude smaller than D_{sm}, reflecting the much stronger interaction of the membrane with protein than with solvent.

Diffusion Cell

The analysis of data in the diffusion cell is described in detail in a forthcoming study (4). The most accurate results were obtained by running the experiments for approximately twenty-four hours and then measuring the amount of radiolabeled protein in each chamber. There was some variation in data for different membranes from the same lot, but the results for albumin in NOVA-50 membranes were well represented as $KD_{\text{eff}} = 4 \pm 1 \times 10^{-11}$ cm^2/sec. Data obtained at different total protein concentrations ($x_p + x_{p^*}$) indicate that the last term in Eq. (32) makes a negligible contribution to KD_{eff}, i.e., $KD_{\text{eff}} = KD_2$. These results were also confirmed by evaluating the mutual diffusion coefficient (2) in a system in which one chamber was initially filled with a protein solution and the other side with buffer alone.

The value of KD_2 determined in the diffusion cell is in good agreement with that evaluated in the batch filtration system. The value obtained from the best-fit values of KD_2/D_1 and δ/D_1 in the filtration system is $KD_2 = 3 \pm 0.2 \times 10^{-11}$ cm^2/sec compared to $4 \pm 1 \times 10^{-11}$ cm^2/sec in the diffusion experiments. This agreement demonstrates that these parameters are true membrane parameters, independent of flow rate and experimental

geometry. These results also indicate the general applicability of the Stefan-Maxwell analysis to membrane transport of proteins in a variety of experimental systems. The experimental and theoretical analyses presented here form the basis for continued studies on protein transport in ultrafiltration membranes, in particular studies of protein fractionation using size-selective membranes.

NOTATION

C = concentration
C^+ = asymptotic wall concentration, g/L or moles/L
D = bulk protein diffusion coefficient, cm^2/sec
D_{ij} = Stefan-Maxwell diffusivity, cm^2/sec
D_1 = lumped diffusivity, Eq. (6), cm^2/sec
D_2 = lumped diffusivity, Eq. (7), cm^2/sec
D_{eff} = effective diffusivity, Eq. (32), cm^2/sec
K = equilibrium partition coefficient, dimensionless
L_p = hydraulic permeability, cm/sec/mm Hg
N = molar flux, $moles/cm^2/sec$
P = applied hydrostatic pressure, mm Hg
S_a = apparent sieving coefficient, dimensionless
V = partial molar volume, cm^3/mol
V_{pore} = volume of a membrane pore, cm^3
V' = accessible pore volume, cm^3
v = ultrafiltrate velocity, Eq. (14), cm/sec
x = mole fraction, dimensionless

Subscripts

b = bulk
f = filtrate
m = membrane
p = protein
p^* = radiolabeled protein
s = solvent
w = wall (membrane surface)

Greek Letters

α = parameter in integral solution, Eq. (29), sec/cm
γ = activity coefficient, dimensionless
δ = membrane thickness, μm
π = osmotic pressure, mm Hg
σ = Staverman reflection coefficient, dimensionless

ACKNOWLEDGEMENTS

This work was supported in part by the Shell Faculty Career Initiation Fund and by NSF Grant CBT-8708871. The authors wish to acknowledge Filtron Corporation for their generous donation of the NOVA membranes and Sharon Bickle for her assistance in the lab.

REFERENCES

1. B.C. Robertson and A.L. Zydney, *Trans. Am. Soc. Art. Intern. Organs*, 10, 118, (1987).
2. K.H. Keller, E.R. Canales, S.I. Yum, *J. Phys. Chem.*, 75, 379 (1971).
3. E.M. Scattergood and E.N. Lightfoot, *Trans. Far. Soc.*, 64, 1135 (1968).
4. B.C. Robertson and A.L. Zydney, *J. Mem. Sci.*, in preparation (1988).
5. A. Katchalsky and P.F. Curran, *NonEquilibrium Thermodynamics in Biophysics*, Harvard University Press, Cambridge, Mass. (1967).
6. K.S. Spiegler and O. Kedem, *Desalination*, 1, 311 (1966).
7. E.N. Lightfoot, *Transport Phenomena and Living Systems*, Wiley, New York (1974).
8. P.C. Lewellen, *Hydrodynamic Analysis of Microporous Mass Transport*, PhD Thesis, University of Wisconsin, Madison, WI, (1982).
9. E.J. Hellund, *Phys. Rev.*, 57, 319 (1940).
10. J.O. Hirschfelder, C.F. Curtiss, and R.B. Bird, *Molecular Theory of Liquids and Gases*, Wiley, New York (1964).
11. B.C. Robertson, *A Mass Transfer Analysis of Selective Protein Filtration with Applications to Plasma Exchange Therapy*, PhD Thesis, University of Delaware, Newark, DE, (1988).
12. M.J. Lysaght and M. Schmidt, in Artificial Organs: The W. J. Kolff Festschrift, VCH Publishers, Inc., Florida (1987).
13. V.L. Vilker, C.K. Colton, and K.A. Smith, *J. Colloid Inter. Sci.*, 79, 548 (1981).
14. E.D. Glandt, *AIChE J.*, 27, 51 (1981).
15. V.L. Vilker, C.K. Colton, and K.A. Smith, *AIChE J.*, 27, 637 (1981).